

Improved mid-infrared cross-sections for peroxyacetyl nitrate (PAN) vapour

G. Allen¹, J. J. Remedios¹, D. A. Newnham^{2,*}, K. M. Smith², and P. S. Monks³

¹EOS, Space Research Centre, Department of Physics and Astronomy, University of Leicester, Leicester, LE1 7RH, UK

²Space Science and Technology Department, Rutherford Appleton Laboratory, Didcot, Oxon, OX11 0QX, UK

³Department of Chemistry, University of Leicester, Leicester, LE1 7RH, UK

* now at: TeraView Limited, Platinum Building, St John's Innovation Park, Cambridge, CB4 0WS, UK

Received: 8 July 2004 – Published in Atmos. Chem. Phys. Discuss.: 22 September 2004

Revised: 4 January 2005 – Accepted: 5 January 2005 – Published: 17 January 2005

Abstract. Absorption spectra of peroxyacetyl nitrate (PAN, $\text{CH}_3\text{C}(\text{O})\text{OONO}_2$) vapour at room temperature (295K) have been measured in the mid-infrared range, 550–2200 cm^{-1} (18.2–4.55 μm), using a Fourier Transform infrared spectrometer at instrument resolutions of 0.25 and 0.03 cm^{-1} (unapodised). Between five and eight measurements were obtained for each spectral band of PAN in the pressure range 0.24–2.20 mb showing good agreement with Beer's law. Both cross-section data and integrated absorption intensities for the five principal bands in the PAN spectra in this spectral range have been derived with peak cross-sections of the 794, 1163, 1302, 1741 and 1842 cm^{-1} bands measured to be 0.95(± 0.02), 1.21(± 0.03), 0.92(± 0.02), 2.39(± 0.06) and 0.74(± 0.03) ($\times 10^{-18}$ cm^2 molecule $^{-1}$) respectively. Band intensities and band centre absorptivities are also reported for four weaker PAN absorption bands in the mid infrared for the first time. These observations are the highest spectral resolution measurements of PAN bands reported in the infrared to date. For three of the five strongest bands, the absolute integrated absorption intensities are in excellent agreement with previous studies. A 4.8% lower integrated intensity was found for the 1741 cm^{-1} $\nu_{as}(\text{NO}_2)$ PAN absorption band, possibly as a result of the removal in this work of spectra affected by acetone contamination, while a 10.6% higher intensity was determined for the 1163 cm^{-1} $\nu(\text{C}-\text{O})$ absorption band. No resolution of fine structure in the PAN absorption bands was observed at the resolutions studied. The confirmation of absorption cross-sections and estimated errors in this work will allow more accurate investigations of PAN using infrared spectroscopy, particularly for remote sensing of PAN in the atmosphere.

1 Introduction

Peroxyacetyl nitrate (PAN) is an important atmospheric trace species through its role as a reservoir of the active nitrogen compound, NO_2 , and through its impact on the oxidising potential of the atmosphere. The PAN compound is formed in the atmosphere by the oxidation of acetaldehyde and further reaction with nitrogen dioxide (Singh, 1987). In the atmosphere, the highest concentrations of PAN are often found in so-called photochemical smog episodes, such as Los Angeles smog events where it was first noted by Stephens (1956). The chief loss mechanism for PAN in the lower troposphere is thermolysis, which occurs readily at temperatures above 273 K with a PAN lifetime of a matter of hours (Kirchener et al., 1999). However, this thermolysis rate drops quickly with temperature allowing lifetimes in the order of months against thermolysis in the cold upper troposphere (of order 200 K). In this region of the atmosphere, the photolysis rate becomes dominant and hence the species can be an important indicator of the photochemical age of polluted airmasses. The long lifetime of PAN in the upper troposphere allows it to transport NO_2 over wide areas, taking NO_2 from polluted regions and releasing it in remote pristine locations where active nitrogen chemistry can influence the production of surface ozone (Olszyna et al., 1994). PAN concentrations as high as 650 pptv are regularly seen in pollution plumes such as those observed by Roberts et al. (2004) in Asian plumes as part of the Intercontinental Transport and Chemical Transformation 2002 (ITCT 2K2) project.

It has now become clear that PAN is one of the most important reservoirs of active nitrogen in the troposphere and, in some regions, is the dominant form of odd nitrogen, NO_y (where $\text{NO}_y = \text{NO} + \text{NO}_2 + \text{reservoir compounds}$). PAN also has an effect on the oxidising power of the atmosphere through its reaction with the hydroxyl radical, OH (Talukdar et al., 1995). In the atmosphere, PAN has only been

Correspondence to: G. Allen
(ga15@le.ac.uk)

Table 1. Configuration of the Bruker IFS120 HR spectrometer for PAN vapour sample measurements.

Spectrometer Configuration	
Resolution (nominal)	0.03/0.25 cm ⁻¹
Beamsplitter	Ge/potassium bromide (KBr)
FTIR input aperture	1.0 mm
Detectors	Broadband liquid nitrogen-cooled mercury cadmium telluride (MCT-D316),DLaTGS
Source	Globar
Gas cell	26.1 cm glass (evacuatable)
Cell windows	Wedge KBr

measured by in situ studies such as those made by Gas Chromatography Electron Capture Detection (GC-ECD) techniques (Tanimoto et al., 1999) during aircraft campaigns such as those detailed by Emmons et al., (1997). The typically low concentrations of PAN (<100 pptv) make it difficult to detect by these methods and errors remain high (typically 30%), with a limit of detection of around 50 pptv. New satellite missions could provide an alternative means to remotely detect trace organic species on a global scale through their characteristic infrared signature. The Michelson Interferometer for Passive Atmospheric Sounding (Nett et al., 2001) onboard the European Space Agency's Envisat platform (Louet, 2001) launched in March 2002, is one such instrument to exploit the potential of using infrared limb emission spectra measured at high spectral resolution to retrieve profile information for trace atmospheric species (Fischer and Oelhaf, 1996).

The retrieval of concentration data from satellite-derived spectra requires accurate reference cross-sections measured in the laboratory at sufficiently high spectral resolution. The high resolution is important for two reasons: 1) accurate calculation of radiative transfer in the atmosphere requires knowledge of spectroscopic behaviour to within the typical separations of overlapping lines (less than 0.1 cm⁻¹ for the troposphere where PAN is important); 2) the MIPAS instrument has an unapodised spectral resolution of 0.025 cm⁻¹ and is therefore sensitive to spectral detail at this level. Thus appropriate data for PAN is a prerequisite for studies to examine the spectral signature of this gas in infrared remote sensing data.

In this paper, we report the first data for the infrared absorption cross-sections of PAN vapour to be obtained at spectral resolutions greater than 0.1 cm⁻¹. The new spectral data for PAN will allow greater confidence in identification of PAN effects in infra-red spectra ranging from the MIPAS example discussed here to air quality measurements to laboratory investigations of PAN and related compounds.

It is not possible to yet ascribe general detection limits for PAN by FTIR remote sensing due to the variability in FTIR

instrument performance (e.g. resolution and sample path-length), however the 794 and 1163 cm⁻¹ absorption bands of PAN are likely to be of particular interest for remote sensing applications as these spectral regions are not saturated by strong atmospheric absorbing compounds such as water vapour in the upper tropopause (8–15 km) region.

2 Experimental details

The spectra presented here were recorded using the Bruker IFS 120HR Fourier transform infrared (FTIR) spectrometer at the Molecular Spectroscopy Facility, Rutherford Appleton Laboratory, UK. The configuration of the instrument for the measurements reported here is listed in Table 1. A Fourier Transform spectrometer is employed here for its ability to simultaneously measure the wide spectral range required for the broad absorption bands of PAN (typically greater than 40 cm⁻¹). The IFS 120 HR spectrometer is noted to give excellent radiometric accuracy in comparison to other FTIR instruments and is not observed to be subject to significant error such as the warm aperture problem (Johnson et al., 2002). The apparatus consisted of an evacuated 26.1 cm path length glass absorption cell equipped with potassium bromide windows interfaced to a customised gas handling vacuum line.

Three overlapping spectral regions in the mid-infrared were measured using appropriate optical and electronic filters. The use of optical filters covering a narrow spectral range improves signal to noise and together with the choice of a small stop aperture (1.0 mm) and electronic filter, greatly reduces the effects of detector non-linearity. Such non-linearity is manifest by the presence of a detected signal outside of the spectral region permitted by the optical filter or detector passband. No such signal was observed in any of the measurements reported in this paper. It was decided to remove the effects of non-linearity in this study, rather than to attempt removal of such errors later.

Both DLaTGS and liquid nitrogen cooled MCT detectors were used, giving excellent signal to noise over the region of interest (typically better than 500:1 after co-addition at 1740.5 cm⁻¹ and 450:1 at worst for the 794.0 cm⁻¹ band). Of the measurements employed in the data analysis, a total of eight spectra were measured in the 550–1650 cm⁻¹ region (five measurements at 0.25 cm⁻¹ and three at 0.03 cm⁻¹ resolution) and five observations of the 1650–2200 cm⁻¹ region (two measurements at 0.25 cm⁻¹ and three at 0.03 cm⁻¹ resolution). Measurements made at 0.25 cm⁻¹ and 0.03 cm⁻¹ resolution took approximately six minutes and sixteen minutes respectively. Spectra were successfully recorded over a pressure range of 0.24–2.20 mb and employed in the data analysis to obtain absorptivities and integrated intensities. In our experiment, pressures greater than this were not used due to an inability to obtain large quantities of PAN from individually prepared samples. However, this limit does have the

Table 2. Spectral fitting ranges for retrieval of contaminant gas concentrations for carbon dioxide and water vapour.

Species	Window 1 range/cm ⁻¹	Window 2 range/cm ⁻¹	Window 3 range/cm ⁻¹
CO ₂	643–697	2255–2385	3560–3750
H ₂ O	1465–1575	1480–1625	

advantage that PAN bands do not approach saturation (>20% transmission for the 1741 cm⁻¹ at 2.20 mb).

The possible effects of sample emission (Ballard et al., 1992) were also investigated by recording background spectra with the global source switched on and at room temperature. No significant sample emission effect was observed.

Pressure was monitored throughout the measurements by calibrated 10 Torr and 1000 Torr MKS Baratron 390 pressure gauges (1 Torr=1.33 mb). To avoid decomposition or detonation of the PAN sample, the Baratron gauges were operated at room temperature rather than at the normal 40°C thermostated operating temperature. At the air-conditioned laboratory temperature of 295±1 K, the uncertainty in the 10 Torr Baratron calibration was determined to be small (less than 0.7% of full scale) by cross-calibration between the thermostated and non-heated Baratron gauges. No observable drift was seen between the gauges over a period of two hours with a static nitrogen sample.

The small leak rate of air into the absorption cell via the vacuum line was periodically measured and included in the procedure for calculating the partial pressure of PAN employed in calculating the final cross-section. This leak rate was measured to be small (less than 0.001 mb/minute). Over the course of a typical measurement (approximately six minutes), such a leak is of little significance to the sample pressure studied, but is included as an error for completeness.

Cell temperature was monitored by a series of eight platinum resistance (PT100) thermometers, with a typical mean accuracy of 0.1 K, attached in thermal contact with the external walls of the absorption cell.

The recorded spectra were averaged from 50 co-added scans at unapodised resolutions of 0.25 and 0.03 cm⁻¹ (where resolution is defined here as 0.9/maximum optical path difference) and apodised with the Norton-Beer strong function (Norton and Beer, 1976, 1977). Transmission spectra were calculated by ratioing PAN sample spectra with the average of background spectra recorded immediately before and after each sample measurement. PAN samples were prepared by the nitration of peracetic acid in the following synthesis based on the method detailed by Gaffney et al. (1984) and Nielsen et al. (1982). Peracetic acid (30% w/v) was first prepared by the equilibrium reaction between hydrogen peroxide (30% w/v), sulphuric acid (99.999% w/v) and glacial acetic acid. The peracetic acid mixture was then added slowly to a mixture of dodecane (cooled to 1–3°C), fuming nitric acid and sulphuric acid (99.999% w/v). The

organic product was dried with anhydrous magnesium sulphate and dissolved in dodecane. The success of the synthesis was tested spectroscopically for the first samples using a low-resolution Perkin-Elmer FTIR spectrometer and purity of PAN-dodecane samples were measured by Gas Chromatography to be greater than 99%.

The preparation of pure gaseous PAN samples is hazardous owing to the inherent explosive and toxic nature of the compound and required a dedicated system for gas handling. The PAN gas was extracted from the dodecane solvent using liquid nitrogen freeze-pump-thaw cycles on a high vacuum line. Due to the potential for errors arising from chemical loss rates of PAN to thermolysis and photolysis, samples were transferred to the absorption cell as quickly as possible after isolation from the solvent.

3 Error analysis

A number of weak spectral signatures due to contaminants were identified in some measurements. Despite several attempts to remove sample contaminants, small amounts of water vapour, carbon dioxide and nitrogen dioxide were observed in two spectra used in this paper. These spectra are included in this paper as it was possible to accurately quantify the concentration of contaminants and remove their spectral absorption through spectral fitting. The removal procedure adopted varied according to whether the spectral contamination was in the form of spectral lines or broad absorption bands.

Once the contaminant signatures have been removed, absolute absorption cross-sections can be calculated using the Beer-Lambert law

$$I = I_0 e^{(-n\sigma x)} \quad (1)$$

where n is the target gas number density (molecules m⁻³), σ is the absorption cross-section (cm² molecule⁻¹) and x is the absorption cell path length (m). The I/I_0 term represents the transmission spectra recorded in the experiment.

Contaminant partial pressures for CO₂ and H₂O (where observed) were subtracted from the measured cell pressure before calculation of PAN cross-sections, absorptivities and integrated intensities. Other sources of error were also considered before determining the PAN concentration including the small contribution of air leaks to the measured pressures and the small rate of decrease in PAN concentration. Table 3

Table 3. Source and magnitude of typical errors assigned to measurements made in this study. The range in uncertainty reflects the range of error assigned for different samples.

Error Source	Sample pressure uncertainty/mb	Radiometric uncertainty (converted to absorbance units)
Cell leak	0.006–0.03	–
PAN adsorption in cell	0.01–0.035	–
PAN decomposition	0.005–0.02	–
Temperature drift	0.000–0.001	0.001
Pressure gauge uncertainty	0.01–0.15*	–
Sample contamination	0.001–0.1*	–
Instrumental noise	–	0.001

*For the highest PAN sample pressures (2.2 mb).

lists the typical magnitudes of such sources of error. In most cases, the errors in Table 3 correspond to an uncertainty in the PAN concentration, whilst instrumental error corresponds to a radiometric error.

There remains the possibility of the presence of non-infrared active gas species in the sample that are not introduced by air leaks but through release of such gases dissolved in the dodecane. Such errors would be systematic for all bands in individual recorded spectra but can vary from sample to sample. However, since relative band intensities are derived from linear fits (see later), the resulting error on, for example, integrated band intensities is always to systematically decrease the derived cross-section and to introduce random uncertainty into the line fit results.

3.1 Line contaminants

Carbon dioxide (CO₂) along with other products of thermal decomposition (Miller et al., 1999; von Ahsen and Willner, 2004) is produced by the breakdown of PAN during storage and sample preparation. Thermolysis products other than carbon dioxide, such as methyl nitrate (CH₃ONO₂), are not observed in the measured sample as no characteristic spectral absorption of such products was observed. In performing simulations for the amounts of methyl nitrate and other products that would be required to be distinguishable from baseline noise we have found that this limit is less than 100 ppmv and therefore negligible.

Various methods were employed to reduce sample impurities. Freshly prepared samples gave the best results, with negligible carbon dioxide levels. Long-term storage of prepared samples of over a week led to greater levels of impurity. Opaque black shielding around the apparatus reduced photolysis of PAN, which could produce nitrogen dioxide and N₂O₄. Care was taken to ensure as complete as possible drying with magnesium sulphate during synthesis.

The effect of contaminants on the determination of absorption cross-sections is two-fold. Firstly, the contribution to the number density term in Eq. (1) from the con-

taminants must be removed. Secondly, the measured spectra should be corrected for the presence of contaminant spectral lines. The concentration, and hence number density contribution from line contaminants, was calculated by fitting the contaminant spectral lines using an optimal estimation technique described by Rodgers (2000), which provides a non-linear inverse fitting technique with mathematical error estimation. The spectral ranges used for this fitting method are shown in Table 2. Line parameters for the contaminating gases were obtained from the HITRAN 2000 database (Rothman, 1992, 2003) and modelled spectra were produced using the Oxford Reference Forward Model described by Dudhia (<http://www.atm.ox.ac.uk/RFM>).

The residuals to spectra fitted in this way showed excellent results with uncertainty in contaminant concentrations of no more than 100 ppmv (0.1% of sample pressure).

3.2 Broadband contaminants

An ambiguity in the relative intensity of the 1741 cm⁻¹ ($\nu_{as}(\text{NO}_2)$) PAN band in initial tests led to the conclusion that a number of spectra included subtle signatures of acetone vapour. The acetone spectrum includes a band of broad shape centred also at 1741 cm⁻¹. It should be noted that measurements exhibiting acetone contamination (deduced by ratioing against a spectrum known to be free from acetone contamination at 1220 cm⁻¹) were discarded from the calculation of cross-sections and all other data reported in this paper. We discuss its significance here as it may have relevance to previously reported PAN data.

Acetone (CH₃C(O)CH₃) may be a product of reactions both in the stored sample and in the gas phase and may also be present during synthesis and hence dissolved with PAN in dodecane at this point. No other contaminant spectral features were observed other than those already discussed, with the exception of trace quantities of NO₂ in some early samples, which is another product of PAN thermolysis (Bruckmann and Willner, 1983; von Ahsen and Willner, 2004).

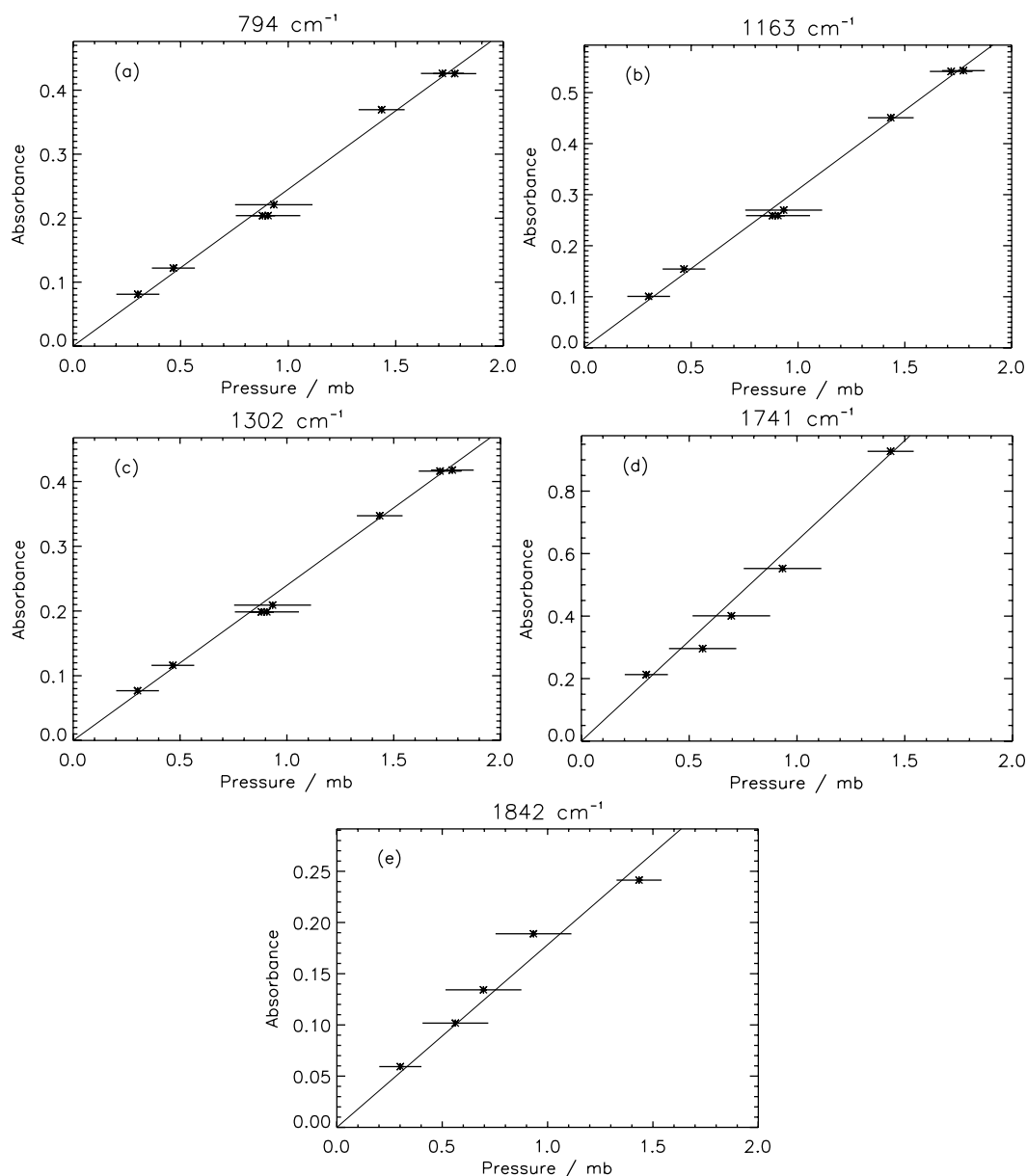


Fig. 1. Infrared absorptivities taken at the quoted band centre as a function of PAN pressure for (a) 794 cm^{-1} , 8 samples, (b) 1163 cm^{-1} , 8 samples, (c) 1302 cm^{-1} , 8 samples, (d) 1741 cm^{-1} , 5 samples and (e) 1842 cm^{-1} , 5 samples. Errors shown represent the total error assigned for each sample measurement.

4 Results and discussion

It should be noted that measurements reported in this paper were conducted for samples of reasonably pure PAN vapour only and no effects of pressure broadening are discussed. Measurements recorded at 0.25 and 0.03 cm^{-1} resolution were compared with no differences observed in the resolution of fine structure or changes in absorption peak intensity. Very high-resolution measurements (greater than 0.005 cm^{-1}) were not attempted in this study due to concerns over the stability of the sample over longer measurement times (greater than 1 h).

Infrared absorptivities are determined from the slope of error weighted linear least squares regression fits to $A=f(P)$, where A is absorbance and P is pressure (Fig. 1). Similarly, integrated band intensities are calculated from such fits to integrated band area (see Fig. 3). As PAN absorption bands do not approach saturation in these measurements, this error weighting method was considered to be more reliable in calculating such fits to Beer's law, rather than using the transmission weighting approach described by Chu et al. (1999) for bands that approach saturation.

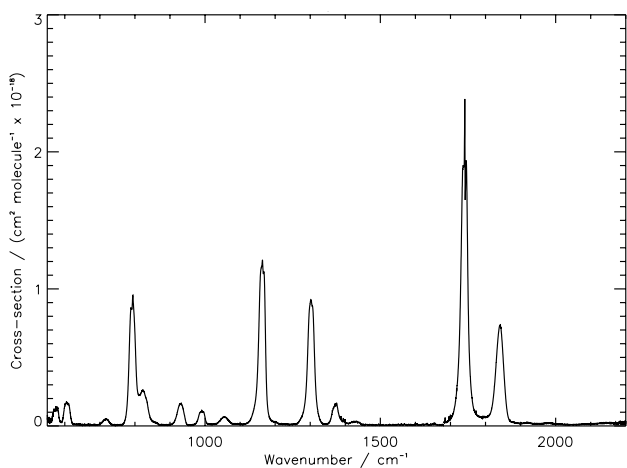


Fig. 2. PAN absorption cross-section derived from Beer's law fitting of 8 samples in the 550–1650 cm^{-1} spectral region and 5 between 1650–2200 cm^{-1} . Temperature = 295 K \pm 1 K, unapodised resolution = 0.25 cm^{-1} .

4.1 Infrared absorptivities

Figure 1 shows peak absorbances measured for each of the five principal PAN bands plotted against determined PAN partial pressure. Absorbance is calculated as usual as the negative logarithm to the base 10 of the transmission, defined in Sect. 3. Work by Tsalkani and Toupance (1989), on determining infrared absorptivities for the same five absorption bands over a pressure range of 0.40 to 11.61 mb showed linearity of Beer's law. This work, although over a smaller pressure range, also confirms this linearity over the pressure range 0.24–2.20 mb.

The individual error bars plotted in Fig. 1 represent the sum of all errors assigned for each sample (See Table 3 for typical sources of such error). The uncertainties in PAN concentration and radiometric accuracy are represented on the x and y-axis respectively. For the data points with largest error, the pressure gauge uncertainty and contaminant uncertainty are the dominant factors.

There is very little scatter around the fitted regression lines, although two experimental points are not fitted within the known error budget in the 794 ($\delta(\text{NO}_2)$), 1163 ($\nu(\text{C-O})$) and 1302 cm^{-1} ($\nu_s(\text{NO}_2)$) bands. The small radiometric error represented as an error bar on the y-axis of Fig. 1 is not observable on the scale of the figure. Infrared absorptivities derived from these fits for band centres of the five principal PAN bands are shown in Table 4 with a comparison to previous studies. The quoted errors represent a two standard deviation (95% confidence level) obtained from the fit statistics to each Beer's law fit in Fig. 3. The first reported absorptivities for four of the weaker PAN bands in the mid infrared are also calculated from the same spectra and are also shown in Table 4. There is excellent agreement in Table 4 for the 794, 1163 and 1302 cm^{-1} bands with respect

to work by Tsalkani and Toupance (1989) and by Niki et al. (1985). However, a significant difference exists between the datasets for the 1842 cm^{-1} band with a 15% difference with the Tsalkani and Toupance (1989) result and 7% with that reported by Niki et al. (1985). The reason for this difference is unclear. The higher absorptivities reported for the 1741 cm^{-1} PAN band in earlier studies at lower resolutions could be subject to interference from a noted contaminant water vapour absorption line centred at 1739.850 cm^{-1} . This contaminant absorption line would not be resolved from the 1741 cm^{-1} PAN band centre at spectral resolutions below 0.5 cm^{-1} such as those resolutions employed by all but Niki et al. (1985) and in this work. Some water vapour contamination was noted in those studies detailed in Table 4. This interference could contribute positively to the calculated absorptivity in low-resolution studies giving positively biased data for the absorptivity of the 1741 cm^{-1} band.

A detailed comparison could also be performed for integrated intensities. This quantity, in principle, is not subject to resolution effects as the bandwidth considered is suitably large relative to the resolution so long as there is no spectral saturation present.

4.2 Cross-section calculation

Figure 2 shows the PAN cross-section derived from the fit to Beer's law for all sample measurements for each spectral point. The resultant PAN cross-section exhibits an excellent zero baseline reflecting the quality of the instrument and detectors used for this investigation. The band centre positions are in excellent agreement with those reported for PAN in previous studies (Stephens, 1969; Gaffney et al., 1984; Bruckmann and Willner, 1983; Niki et al., 1985; Tsalkani and Toupance, 1989). We use the band assignments for PAN previously reported by Gaffney et al. (1984) and Bruckmann and Willner (1983).

Peak cross-sections of the five principal PAN absorption band centres are calculated to be 0.95(\pm 0.02), 1.21(\pm 0.03), 0.92(\pm 0.02), 2.39(\pm 0.06) and 0.74(\pm 0.03) ($\times 10^{-18} \text{ cm}^2 \text{ molecule}^{-1}$) for the 794, 1163, 1302, 1741 and 1842 cm^{-1} bands respectively. The errors quoted represent the two standard deviation error calculated from Beer's law fits at the band centres.

The low noise level of the FTIR cross-section shown in Fig. 2 allows the very weak 590 cm^{-1} (ν_{22}), 720 cm^{-1} ($\text{wag}(\text{NO}_2)$) and 1375 cm^{-1} ($\delta_s \text{CH}_3$) bands to be observed. However, these bands are not easily analysed here because of detector cut-off and associated noise, signal-to-noise ratio, and the complexity of the band structure respectively. Hence results here are limited to the five main bands and to the weaker 606, 930, 991 and 1055 cm^{-1} bands.

The observation of a Q-branch in the 1741 cm^{-1} PAN band may be of interest in remote sensing applications. The full width at half maximum of this spectral feature was measured to be 1.4 cm^{-1} , peaking at 1740.8 cm^{-1} , whilst

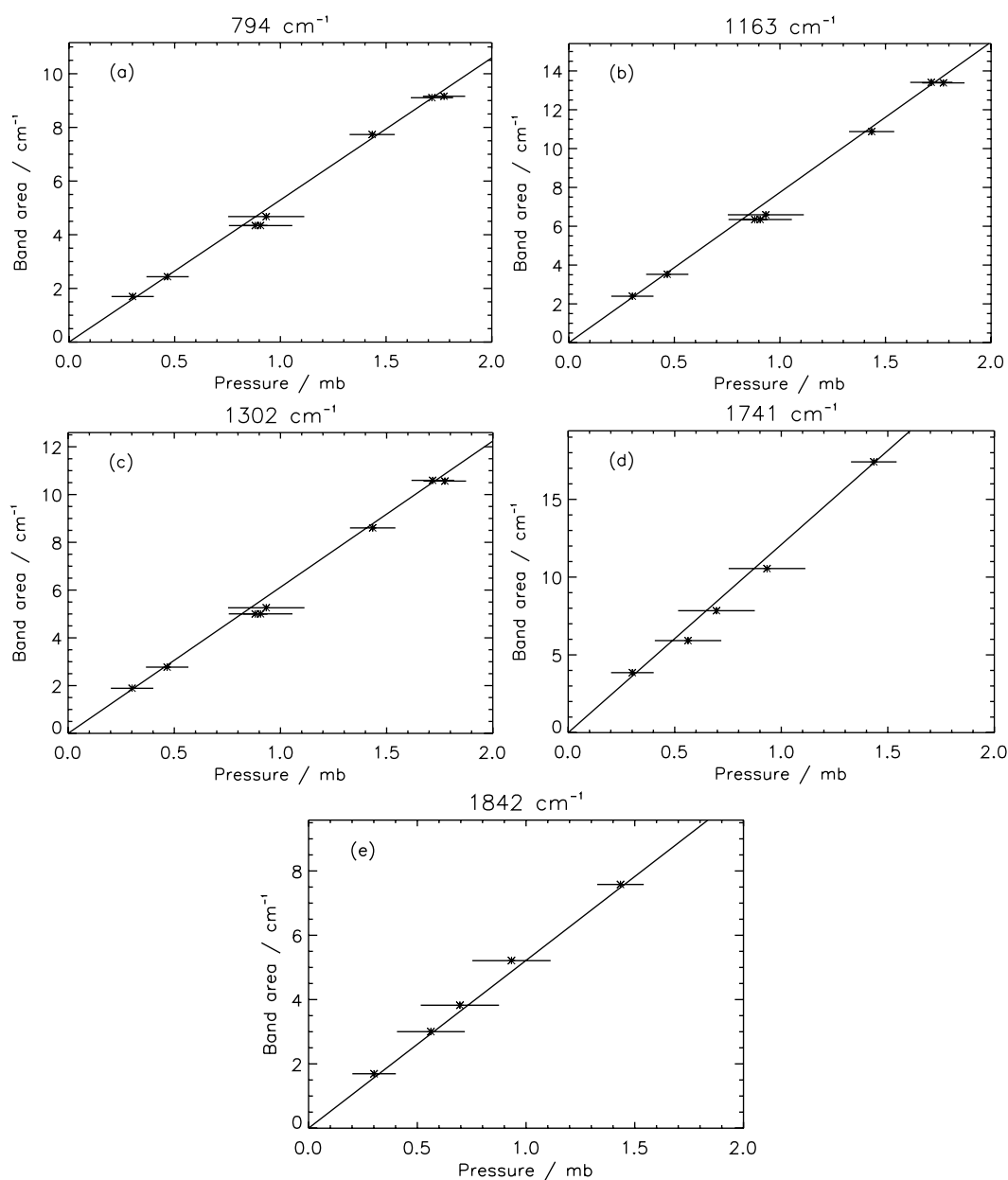


Fig. 3. Integrated PAN band areas calculated as a function of PAN pressure for (a) 794 cm^{-1} , 8 samples, (b) 1163 cm^{-1} , 8 samples, (c) 1302 cm^{-1} , 8 samples, (d) 1741 cm^{-1} , 5 samples and (e) 1842 cm^{-1} , 5 samples. Errors shown represent the total error assigned for each sample measurement.

its infrared absorptivity is that listed in Table 4 for the 1741 cm^{-1} band centre.

4.3 Integrated band intensities

Integrated band intensities for the five main bands of PAN were determined by summing the absorbances over the spectral ranges detailed in Table 5. The integrated band area for the 794 cm^{-1} absorption band, which interferes with a

smaller band centred at 822 cm^{-1} , is calculated using a vertical truncation at the absorbance minimum between the 794 and 822 cm^{-1} bands.

The results plotted in Fig. 3 show excellent internal consistency given the low partial pressures and limited pressure range of PAN measured. Again, only small scatter around the calculated regression fits is observed although some points remain unfitted within the known error budget. The integrated absorption intensities were again determined from

Table 4. Infrared absorptivities for gaseous PAN ($10^{-1} \mu\text{mol mol}^{-1} \text{m}^{-1}$, log to base 10 to 3 s. f., values refer to 1013.25 mb)* for nine PAN absorption bands with a comparison to previously reported data. Errors for previously reported data have been modified to reflect a two standard deviation, in line with those quoted for this work.

Band centre/ cm^{-1}	Stephens, 1964 Res.: $>5.0 \text{cm}^{-1}$	Bruckmann and Willner, 1983 Res.: 1.20cm^{-1}	Niki et al., 1985 Res.: 0.06cm^{-1}	Tsalkani and Toupance, 1989 Res.: 1.0cm^{-1}	This Work Res.: $0.03/0.25 \text{cm}^{-1}$
606	–	–	–	–	1.55 ± 0.12
794	10.1	13.4	11.5 ± 0.6	12.2 ± 0.4	11.4 ± 0.8
930	–	–	–	–	1.46 ± 0.12
991	–	–	–	–	1.03 ± 0.08
1055	–	–	–	–	0.62 ± 0.06
1163	14.3	15.8	14.5 ± 1.4	15.7 ± 0.6	14.6 ± 1.0
1302	11.2	13.6	11.3 ± 1.2	11.9 ± 0.4	11.4 ± 0.8
1741	23.6	32.6	31.0 ± 3.2	31.4 ± 1.6	30.2 ± 3.0
1842	10.0	12.4	10.2 ± 1.0	10.9 ± 0.4	9.5 ± 1.2

* Note: $1 \mu\text{mol mol}^{-1} = 1 \text{ppmv}$

Table 5. Spectral ranges used to calculate integrated band areas for the nine PAN absorption bands studied.

Band centre position / cm^{-1}	Integration range / cm^{-1}
606	585.0–652.0
794	767.4–810.2
930	900.1–956.0
991	967.5–1008.1
1055	1035.0–1075.1
1163	1115.3–1210.2
1302	1260.7–1333.0
1740	1685.8–1780.0
1842	1802.0–1875.3

the slopes of the least squares linear regression fits and are compared with data from previous studies in Table 6. The errors in Table 6 again represent two standard deviations (95% confidence level) obtained from the fit statistics from Fig. 3. Integrated intensities for the weaker 606, 930, 991 and 1055 cm^{-1} bands are also shown. Our integrated absorption intensity data compare well with those of Tsalkani and Toupance (1989) with a minimum 0.8% difference in the 794 cm^{-1} absorption band and a maximum 10.6% difference in the 1163 cm^{-1} band. Comparing our data with that originally reported by Gaffney et al. (1984), however, we see differences ranging from 2.5% for the 794 cm^{-1} band and 50.5% for the 1741 cm^{-1} band (see later). Large differences were also reported by Tsalkani and Toupance (1989) in their comparison with the Gaffney et al. (1984) data. The results from this work are therefore in better agreement with those of Tsalkani and Toupance (1989). Firstly, this work has found a 4.8% lower intensity for the 1741 cm^{-1} band. Secondly this work calculates the 1163 cm^{-1} ($\nu(\text{C-O})$) band intensity to be 10.6% higher than the data of Tsalkani and Toupance (1989).

It is possible that there is a small curvature in our data for the 1741 and 1842 cm^{-1} bands in Fig. 3, although its significance cannot be addressed within the error bars.

A constant relative difference between all bands would indicate a systematic error due to incorrect pressure measurements for example as noted by Tsalkani and Toupance (1989), who also noted that there may be impurities in the PAN sample contributing to some bands. Tsalkani and Toupance (1989) assert that their PAN samples were >98% pure as determined by gas chromatography and state that the only contaminants identified were carbon dioxide and water vapour. These contaminants are clearly seen in the Tsalkani and Toupance (1989) spectrum with water lines visible in the 1600–1650 cm^{-1} spectral region, even with a relatively low resolution of 1 cm^{-1} .

An informative way to analyse the effects of any contaminants that may be contaminating a band is to consider the relative intensity of each band with respect to a band which shows the best internal consistency and is known to be free from any contaminants that may be thought to be present. The 794 cm^{-1} absorption band is chosen for this purpose here since it shows the best agreement with previous work; Tsalkani and Toupance (1989) employed the 1842 cm^{-1} band for which some absolute intensity disagreements may still exist. The relative intensities for this work are calculated for each independent measurement and averaged to give the results shown in Table 7. In the table, we show the results of Tsalkani and Toupance (1989) together with their re-evaluation of the Gaffney et al. (1984) data; the relative intensities originally reported by Gaffney et al. (1984) seem to be incorrect.

The largest differences in the relative ratios are seen for the 1741 cm^{-1} PAN band. It is possible on the basis of this result that measurement of the 1741 cm^{-1} absorption band in earlier studies may have been affected by the same contamination by acetone seen in our discarded spectra.

Table 6. Infrared integrated intensities ($\text{atm}^{-1} \text{cm}^{-2}$ to 3.s.f) of nine PAN bands with comparison to previously reported data.. (Units refer to 1 atm at ambient temperature 291 K unless otherwise stated). Errors quoted for this work represent a two standard deviation calculated from regression fits. The nature of errors from previously reported data is unknown.

Band centre/ cm^{-1}	Gaffney et al., 1984	Tsalkani and Toupance, 1989	This Work
606	–	–	34.2 ± 1.4
794	247 ± 6	239 ± 4	241 ± 6
930	–	–	32.2 ± 1.2
991	–	–	20.1 ± 0.8
1055	–	–	16.0 ± 0.8
1163	477 ± 9	322 ± 7	356 ± 8
1302	405 ± 20	270 ± 2	281 ± 6
1741	808 ± 34	563 ± 10	537 ± 10
1842	322 ± 9	262 ± 4	260 ± 6

Table 7. Relative integrated absorption intensities normalised to the 794cm^{-1} band intensity. The quoted data from Gaffney et al. (1984), are based on a re-evaluation of the Gaffney et al. (1984) results performed by Tsalkani and Toupance (1989).

Band centre position/ cm^{-1}	Re-evaluation of data reported by Gaffney et al. (1984)	Tsalkani and Toupance (1989)	This work
794	1.00	1.00	1.00
1163	1.33	1.39	1.47
1302	1.13	1.13	1.16
1741	2.11	2.36	2.23
1842	1.10	1.10	1.08

5 Conclusions

Cross-sections of PAN vapour at spectral resolutions of 0.03cm^{-1} and 0.25cm^{-1} have been determined in the mid-infrared range of $550\text{--}2200 \text{cm}^{-1}$ at 295 K.

Peak cross-sections of the five principal PAN absorption band centres are calculated to be $0.95(\pm 0.02)$, $1.21(\pm 0.03)$, $0.92(\pm 0.02)$, $2.39(\pm 0.06)$ and $0.74(\pm 0.03)$ ($\times 10^{-18} \text{cm}^2 \text{molecule}^{-1}$) for the 794, 1163, 1302, 1741 and 1842cm^{-1} PAN bands respectively.

The 794 and 1163cm^{-1} PAN absorption band absorptivities are calculated with good accuracy in this study ($<7\%$ relative error for both bands at the 95% confidence level) and are of particular interest in FTIR remote sensing of the upper tropospheric region (8–15 km).

Integrated band intensities for the five main bands of PAN are seen to be generally in good agreement with earlier work by Tsalkani and Toupance (1989) supporting these results rather than those of Gaffney et al. (1984). The integrated intensity of the 1163cm^{-1} PAN band is noted to show the greatest inconsistency between the datasets. Most significantly, the requirement for remote sensing applications is the confirmation of cross-sectional data with estimated errors. This work achieves both these advances over previously

reported data for PAN for the first time. The nature of a difference in the integrated intensity reported for the 1741cm^{-1} band in the datasets studied remains unresolved although it is proposed here that contamination by acetone in this band may be a source of error in previous measurements. We believe similar contamination may have resulted in an overestimation of the reported integrated intensity for the 1741cm^{-1} band in previously reported data.

In addition, probable contamination from water vapour and carbon dioxide concentrations were not removed in previous calculations of PAN absorption cross-sections. Spectral fitting and partial pressure correction of contaminants in the Gaffney et al. (1984) and Tsalkani and Toupance (1989) datasets are imperative if these data are to be used in quantitative applications. Without access to previous datasets it is difficult to confirm the effects of contamination on their results.

Finally, new integrated band intensities and band centre absorptivities have been reported in this work for the weak PAN absorption bands centred at 606, 930, 990, and 1055cm^{-1} .

Acknowledgements. The authors wish to thank the Natural Environment Research Council (NERC) for supporting G. Allen through grant ref: NER/T/S/2000/01087, and for access to the Molecular Spectroscopy Facility at the Rutherford Appleton Laboratory (RAL). R. G. Williams is thanked for providing technical support at the Rutherford Appleton Laboratory.

Edited by: J. N. Crowley

References

- Ballard, J., Remedios, J. J., and Roscoe, H. K.: Sample emission effect on spectral parameters, *J. Quant. Spectr.*, 48, 733–741, 1992.
- Bruckmann, P. W. and Willner, H.: Infrared spectroscopic study of peroxyacetyl nitrate (PAN) and its decomposition products, *Envir. Sci. Tech.*, 17, 352–357, 1983.
- Chu, P. M., Grunther, F. R., Rhoderick, G. C., and Lafferty, W. J.: The NIST quantitative infrared database, *J. Res. Nat. I.*, 104 (1), 59–81, 1999.
- Emmons, L. K., Carroll, M. A., Hauglustaine, D. A., Brasseur, G. P., Atherton, C., Penner, J., Sillman, S., Levy II, H., Rohrer, F., Wauben, W. M. F., van Velthoven, P. F. J., Wang Y., Jacob, D. J., Bakwin, P., Dickerson, R., Doddridge, B., Gerbig, C., Honrath, R., Hubler, G., Jaffe, D., Kondo, Y., Munger, J. W., Torres, A., and Volz-Thomas, A.: Climatologies of NO_x and NO_y : a comparison of data and models, *Atmos. Envir.*, 31, 1851–1903, 1997.
- Fischer, H. and Oelhaf, H.: Remote sensing of vertical profiles of atmospheric trace constituents with MIPAS limb-emission spectrometers, *Appl. Opt.*, 35, 2787–2796, 1996.
- Gaffney, J. S., Fajer, R., and Senum, G. I.: An improved procedure for high purity gaseous peroxyacetyl nitrate production: Use of heavy lipid solvents, *Atmos. Envir.*, 18, 215–218, 1984.
- Johnson, T. J., Sams, R. L., Blake, T. A., Sharpe, S. W., and Chu, P. M.: Removing aperture-induced artefacts from Fourier Transform infrared intensity values, *Appl. Opt.*, 41, 2831–2839, 2002.
- Kirchener, F., Mayer-Figge, A., Zabel, F., and Becker, K. H.: Thermal stability of peroxy nitrates, *Int. J. Chem. K.*, 31, 127–144, 1999.
- Louet, J.: The Envisat mission and system, *ESA Bulletin – European Space Agency*, (106), 11–25, 2001.
- Miller, C. E., Lynton, J. L., Keevil, D. M., and Francisco, J. S.: Dissociation pathways of Peroxyacetyl Nitrate (PAN), *J. Phys. Chem. A*, 103, 11 451–11 459, 1999.
- Nett, H., Frerick, J., Paulsen, T., and Levrini, G.: The atmospheric instruments and their applications: GOMOS, MIPAS and SCIAMACHY, *ESA Bulletin – European Space Agency*, (106), 77–87, 2001.
- Nielsen, T.: A convenient method for preparation of pure standards of peroxyacetyl nitrate for atmospheric analyses, *Atmos. Envir.*, 16, 2447–2450, 1982.
- Niki, H., Maker, P. D., Savage, C. M., and Breitenbach, L. P.: An FTIR spectroscopic study of the reactions $\text{Br} + \text{CH}_3\text{CHO} \rightarrow \text{HBR} + \text{CH}_3\text{CO}$ and $\text{CH}_3\text{C}(\text{O})\text{OO} + \text{NO}_2 \leftrightarrow \text{CH}_3\text{C}(\text{O})\text{OONO}_2$ (PAN), *Int. J. Chem. K.*, 17, 525–534, 1985.
- Norton, R. H. and Beer, R.: New apodising functions for Fourier spectrometry, *J. Opt. Soc. A*, 66, 259–264, 1976.
- Norton, R. H. and Beer, R.: New apodising functions for Fourier spectrometry – Erratum, *J. Opt. Soc. A.*, 67, 419, 1977.
- Olszyna, K. J., Bailey, E. M., Simonaitis, and R., Meagher, J. F.: O_3 and NO_y relationships at a rural site, *J. Geo. Res-A.*, 99, 14 557–14 563, 1994.
- Roberts, J. M., Flocke, F., Chen, G., Gouw, J., Holloway, J. S., Hübler, G., Neuman, J. A., Nicks, D. K., Nowak, J. B., Parrish, D. D., Ryerson, T. B., Sueper, D. T., Warneke, C., and Fehsenfeld, F. C.: Measurement of peroxyacetic nitric anhydrides (PANs) during the ITCT 2K2 aircraft intensive experiment, *J. Geophys. Res.*, 109, D23S21, 2004.
- Rothman, L. S.: The HITRAN database, *J. Quant. Spectr.*, 48, 469–507, 1992.
- Rothman, L. S., Barbe, A., Benner, D.C., Brown, L. R., Camy-Peyret, C., Carleer, M. R., K. Chance, K., Clerbaux, C., Dana, V., Devi, V. M., Fayth, A. Flaud, J.M., Gamache, R. R., Goldman, A., Jacquemart, D., Jucks, K. W., Lafferty, W. J., Mandin, J.-Y., Massie, S. T., Nemtchinov, V., Newnham, D. A., Perrin, A., Rinsland, C. P., Schroeder, J., Smith, K. M., Smith, M. A. H., Tang, K., Toth, R. A., Vander Auwera, J., Varanasi, P., and Yoshino, K.: The HITRAN molecular spectroscopic database: edition of 2000 including updates through 2001, *J. Quant. Spectr.*, 82 (1–4), 5–44, 2003.
- Rodgers, C. D.: Inverse methods for atmospheric sounding: Theory and practice (Series on atmospheric, oceanic and planetary physics), World Scientific Publishing, 2000.
- Singh, H. B.: Reactive nitrogen in the troposphere – chemistry and transport of NO_x and PAN, *Envir. Sci. Technol.*, 21, 320–327, 1987.
- Stephens, E. R., Hanst P. L., Dörr, R. C., and Scott, W. E.: Reactions of nitrogen dioxide and organic compounds in air, *Ind. Eng. Chem.*, 48, 1498, 1956.
- Talukdar, R. K., Burkholder, J. B., Schmoltner, A., Roberts, J. M., Wilson, R. R., and Ravishankara, A. R.: Investigation of the loss processes for peroxyacetyl nitrate in the atmosphere: UV photolysis and reaction with OH, *J. Geophys. Res. A.*, 100, 14 163–14 173, 1995.
- Tsalkani, N. and Toupance, G.: Infrared absorptivities and integrated band intensities for gaseous peroxyacetyl nitrate (PAN), *Atmos. Envir.*, 23, 1849–1854, 1989.
- von Ahsen, S. and Willner, H.: Thermal decomposition of peroxyacetyl nitrate $\text{CH}_3\text{C}(\text{O})\text{OONO}_2$, *J. Chem. Phys.*, 121, 2048–2057, 2004.